RPE | Radiation Physics & Engineering
A Peer-Reviewed Journal
Published by K.N. Toosi University of Technology
http://rpe.kntu.ac.ir
Research Article

Radiation Physics and Engineering 2025; 6(2):35–40

Implementation of a control system for a laboratory-scale 1 MeV/25 kW electrostatic accelerator for irradiation experiments

Mahyar Shirshekan*, Oveis Hasanpour, Mohammadhosein Sadafi, Shahin Sanaye Hajari, Amir Mohammadi, Mohammad Nazari, Farshad Ghasemi, Mahdi Asl Beigi

Physics and Accelerators Research School, Nuclear Science and Technology Research Institute, Tehran, Iran

HIGHLIGHTS

- A control system was designed and implemented for a laboratory-scale irradiation accelerator.
- The control system hardware/software implementation and safety interlock logic was described.
- Operational tests on 500 kV/10 mA electron beam has been performed with the implemented control system.

ABSTRACT

This article presents the design and implementation of a control system for a 1 MeV, 25 kW electrostatic accelerator, highlighting its architecture, instrumentation, and operational capabilities. The machine is designed for laboratory-scale irradiation experiments. A monolithic control system architecture was selected for its advantages in centralized data management, ease of maintenance, and simplified user access. The system integrates various subsystems, including a high-voltage rectifier, Hartley-type oscillator, voltage multiplier, electron gun, acceleration section, cooling, and gas handling system. Each of the subsystems are equipped with local and/or central interlocks for enhanced safety. The control software, developed using IEC 61131-3 LADDER language and the graphical programming language "G", provides a user-friendly interface for real-time monitoring and adjustment of operational parameters. Currently operational at 500 kV and 10 mA, the system demonstrates effective electron beam irradiation control, ensuring compliance with radiation safety regulations. Future enhancements are planned to optimize performance and expand functionality for diverse experimental needs.

KEYWORDS

Control system
Accelerator
Electrostatic
Electron Beam

HISTORY

Received: 28 May 2024
Revised: 19 October 2024
Accepted: 12 November 2024
Published: Spring 2025

1 Introduction

The design and construction of a parallel-powered capacitive-coupled electrostatic accelerator is currently underway at the Nuclear Science and Technology Research Institute (NSTRI). The accelerator is undergoing stability tests at 500 kV and 10 mA. A control system has been developed and implemented to ensure the safety and stability of the machine subsystems. These subsystems include a 10 kV DC power source, a high-power 200 kHz oscillator unit, a rectifying structure, a generating voltmeter, an insulating gas injection system, an electron acceleration section, and a beam delivery system (Fig. 1).

In a parallel-fed capacitive-coupled voltage multiplier, a high-power multiplier structure generates voltages reaching several million volts. The structure of the high-voltage multiplier comprises of a distributed capacitance circuit, rectifier stacks, and a dome-shaped terminal. This 500 kV high-voltage multiplier (Fig. 2) consists of a column of semi-cylindrical receiving electrodes (coupling electrodes) positioned between two feeder electrodes (Nazari et al., 2020; Hasanpour et al., 2022). The feeder electrodes are powered by a 10 kV/80 kW silicon-controlled rectifier (SCR) DC power supply and a high-power 200 kHz Hartley-type oscillator, which induce the input voltage to the coupling electrodes through the distributed capacitance.

The induced voltage on each coupling electrode is proportional to the voltage of the feeder electrodes (200 kHz, 100 kV). This induced voltage is then rectified in each stage and since the rectifying elements are connected in series, a multiplied output of 500 kV DC is generated.

*Corresponding author: myshirshekan@aeoi.org.ir

https://doi.org/10.22034/rpe.2024.459998.1196

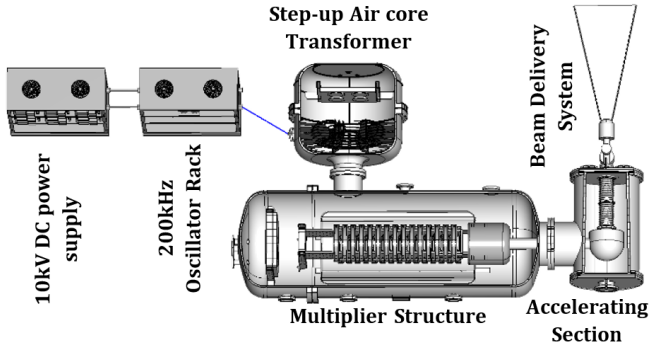

Figure 1: Subsystems of the Parallel-Fed Capacitive Coupled Electrostatic Accelerator.

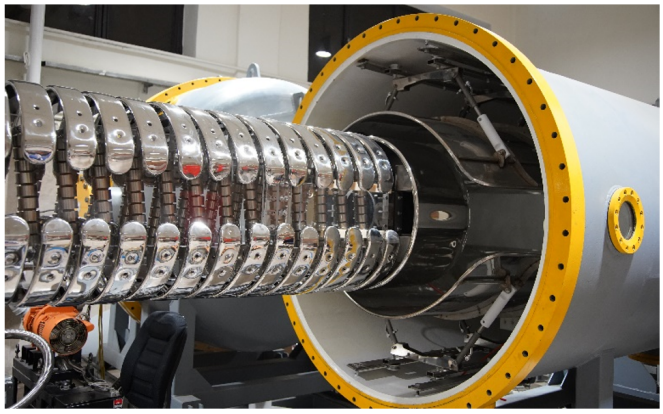

Figure 2: Voltage Multiplier Structure of the Electrostatic Accelerator.

In the acceleration section, an electron beam is produced using a tungsten filament and is accelerated by the 500 kV DC power from the generator section (Nazari et al., 2016a,b). The electron beam, which can deliver power of up to 50 kW, is utilized for applications such as sterilization and polymer cross-linking.

This article presents the implementation of the accelerator control system, which establishes safety interlocks between subsystems and provides monitoring tools for the operation of each subsystem.

2 Control System Architecture

Monolithic and multi-layered architectures are employed for accelerator control systems, each offering distinct advantages (Singh et al., 2010). For the electrostatic accelerator in question, a monolithic architecture was selected based on its size and the type and number of parameters involved. This choice provides several benefits over multi-layered and distributed control systems, including:

- Centralized data storage, which prevents data conflicts and simplifies reporting)
- Easier maintenance and troubleshooting due to a limited number of development platforms
- Reduced response time through the integration of interface and server
- Simplified user access control

A Siemens 315-2PN/DP PLC collects sensor data and forwards user interface commands to actuator devices. Figure 3 illustrates the control system architecture of the electrostatic accelerator.

The implemented architecture ensures simplicity in maintenance and troubleshooting while complying with Iran radiation protection regulations during research and development activities, which aim to maintain a safe distance for personnel from the radiation source. However, this architecture positions the central processing unit (PLC), shown in Fig. 4, in close proximity to the accelerator, which poses a risk of long-term radiation damage to the units if they are not adequately shielded.

3 Instrumentation and Interlocks

This section describes the acceleration instruments that in directly interact with physical parameters. Two types of interlocks are implemented in the machine: (1) local interlocks and (2) central interlocks. Local interlocks are implemented for individual subsystems, while central interlocks are system-wide and are managed through the central control system.

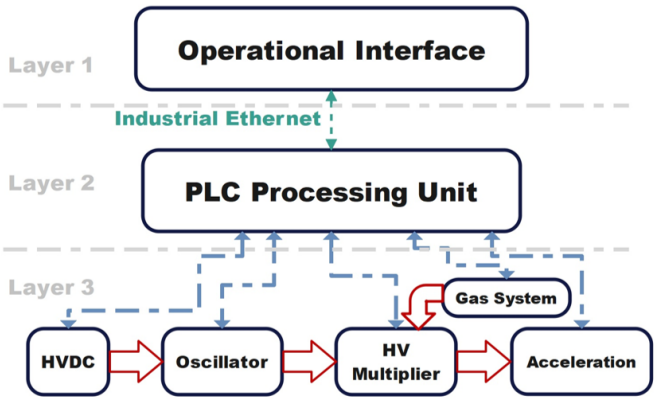

Figure 3: Monolithic Architecture of the Control System.

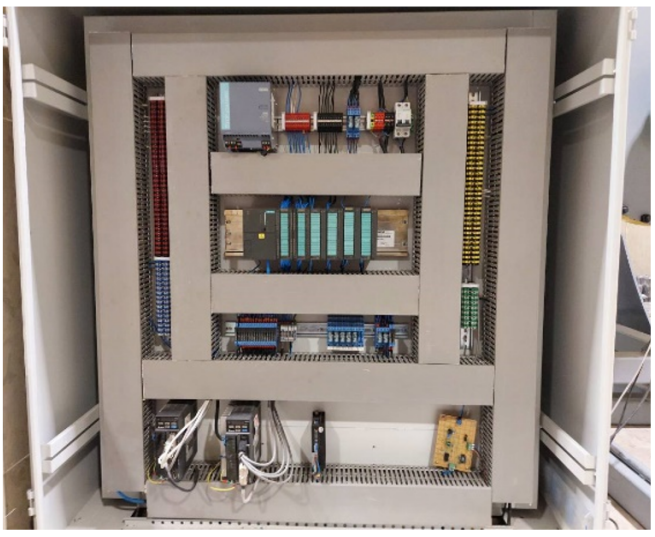

Figure 4: Siemens PLC control rack of the accelerator.

Figure 5: 10 kV/80 kW Silicon-Controlled Rectifier (SCR).

Figure 6: 200 kHz, 10 kV Oscillator Unit.

3.1 Input 10 kV Rectifier Power Supply

The electrostatic accelerator utilizes a 10 kV DC power supply (Fig. 5) to provide bias for the oscillation section. The HVDC power supply consists of two 2.5 kV sections and six 1 kV sections. To achieve the desired set-point voltage, the local control system regulates the output voltage by connecting and disconnecting the DC sections to the output. One of the 1 kV sections is controlled by a thyristor through phase-fired control, allowing for precise voltage regulation.

This unit serves as the input power source for the entire system and provides a safe means to shut down the accelerator. In the event of an emergency or unsafe condition both software and hardware stop commands can be used to disconnect the input HVDC power supply.

The power state (On/Off), output voltage set-point and actual current-voltage status of the unit are controlled and monitored through the control system (Fig. 7).

3.2 High-power Hartley-type Oscillator

To generate a 200 kHz, 200 kV voltage, the Hartley oscillator method is employed, utilizing a GU23A electron tube as the amplifier. This section, illustrated in Fig. 6, features a local controller that automatically adjusts internal parameters automatically after the unit is remotely activated. Continuous monitoring of the tube grid voltage and filament current -essential for ensuring proper operation- is implemented as a part of the operation interface (see Fig. 7).

The operating frequency of the oscillator unit is regulated by its local control system, while the power state of the unit is managed by the central control system. Additionally, the current and voltage status of the high-power amplifier electron tube is continuously monitored in real time (Fig. 7).

3.3 Shutter-type Generating Voltmeter (GVM)

The high-voltage potential of the accelerator is measured using a shutter-type generator voltmeter (GVM), as illustrated Fig. 8. This device features of a shutter mechanism that repeatedly exposes its substrate to the high-voltage, allowing it to measure the induced alternating current. The induced current is proportional to the terminal voltage, enabling the determination of the beam energy (Sadeghche et al., 2023).

In the manufactured GVM (Fig. 8), a servo motor rotates a steel shutter at 3000 rpm. This configuration achieves a measurement resolution of 0.08 kV at 2100 kV. To protect the shutter-shaft connection from abrupt speed changes, a software interlock is implemented.

The data logging panel of the interface (Fig. 9) facilitates the detection of sudden variations in high-voltage and vacuum values.

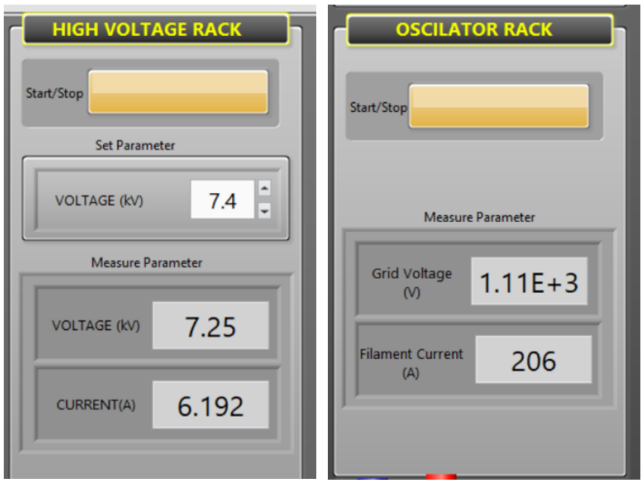

Figure 7: Operational Interface of Input HVDC and Oscillator Unit.

Figure 8: Shutter-Type Generating Voltmeter (GVM).

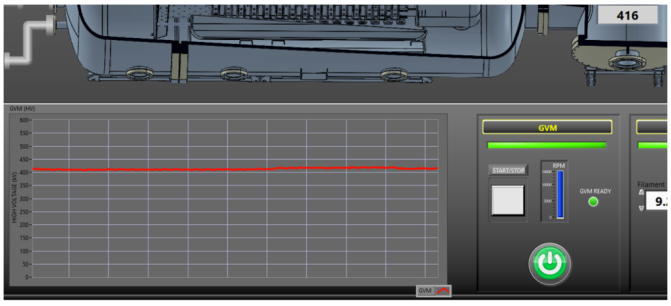

Figure 9: Data-logging Panel of the Accelerating High Voltage.

The rotation speed, operational status (normal or abnormal) of the shutter, and the output signal of the device are processed using calibration coefficients and presented to the user (Fig. 9).

3.4 Insulating Gas Handling System

The gas handling system comprises vacuum pumps, motorized gate valves, pressure sensors, and thermometers. Given that the purity of the insulating gas significantly affects the high-voltage stability of the machine, gas injection occurs when a vacuum level of 10-2 mbar is achieved.

The insulating gas container features glass viewport window, to reduce the risk of personnel injuries, switching from vacuum mode to gas injection mode is performed remotely via motorized gate values. Pressure levels and temperature are continuously monitored to detect gas leaks or anomalies that could compromise insulating performance. A central interlock prevents the increase of the high-voltage in the event of detected anomalies or inadequate pressure is detected.

The set-points and actual states of the motorized gate valves, along with the current insulation pressure or vacuum levels within the container, are continuously monitored and regulated by the central control system.

3.5 Cooling System

A cooling capacity of 25 kW is utilized for dissipation of heat from oscillator and for cooling the insulating gas. The electron tube oscillator is powered by an input of 80kW, operating at an efficiency of 70%, making it the primary source of heat generation of the accelerator.

At elevated temperatures, the N_2/CO_2 insulating gas is less effective in preventing electrical breakdown, and extreme temperature fluctuations can compromise the stability and reliability of the machine. To address this, two heat exchangers are installed in the insulating gas tanks.

The control system incorporates sensors for Total Dissolved Solids (TDS), flow, and temperature sensors to ensure safe operation and prolong the lifespan of the electron tube. The standard TDS level in the inner loop is maintained below 7 ppm to prevent the accumulation of impurities and corrosion of the components, thereby enhancing heat transfer efficiency. The control system monitors the temperature of the insulating gas, the impurity levels of the cooling water, and the operational status of the cooling unit.

3.6 Electron Gun Filament Power Delivery

The electron gun filament power delivery system comprises a Delta ECMA-C20807ES servomotor, which is controlled by a Delta ASDA B2 driver capable of adjusting the rotating speed of an alternator up to 3000 rpm. The speed of the servomotor directly influences the current supplied to the filament, allowing for remote control of the current density of the electron gun via the control system. Figure 10 illustrates the mechanical configuration of the electron gun power delivery system.

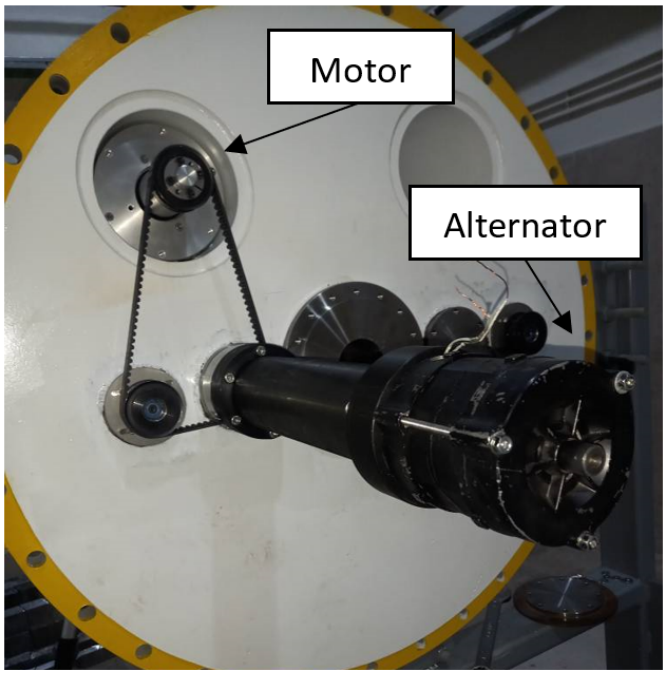

Figure 10: Mechanical Filament Current Control System.

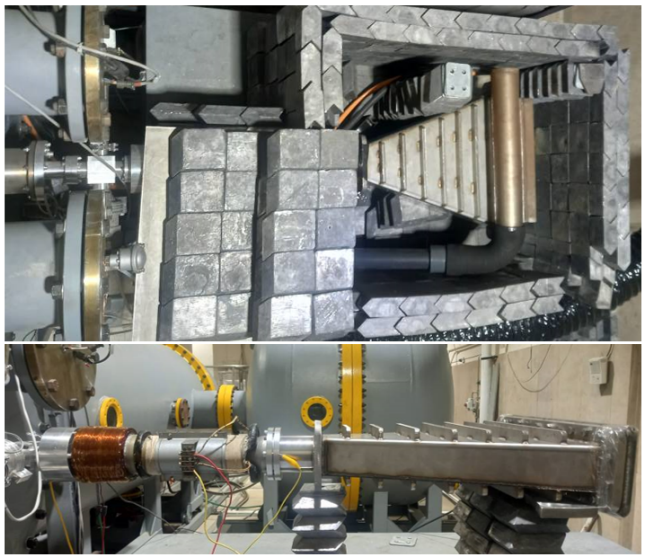

Figure 11: Beam extraction section of the accelerator.

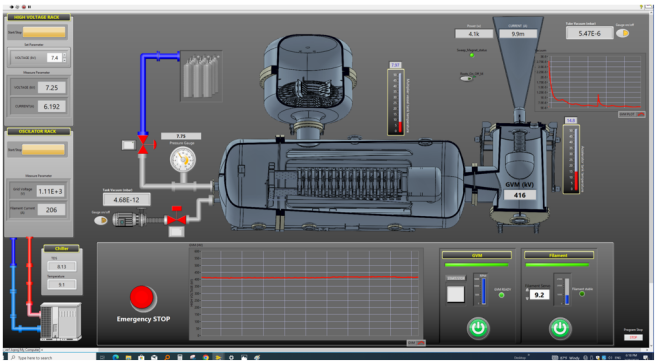

Figure 12: Operational Interface of Accelerator.

3.7 Electron Beam Extraction

The accelerated electron beam is scanned across an 8 cm × 100 cm titanium exit window (Fig. 11). As the machine is designed for laboratory-scale experiments, the frequency, amplitude and waveform of the scanning magnet drive are adjustable.

The operational beam density at the output titanium foil window is 100 μA.cm^{-2} (Kuksanov et al., 2018). To prevent foil failure, the output of the scanning power supplies is continuously monitored by the control system, which includes interlock that halts system operation if the scanning coils current falls below the specified limit.

Currently, a 2 mm thick stainless steel beam catcher serves as a Faraday cup to collect the beam current. The current measured by the Faraday cup and is reported in real time in the operating interface. Once stability tests are successfully completed, the stainless steel beam catcher will be replaced with a 50 μm titanium foil window.

4 Software

The accelerator control system software is designed to effectively manage and regulate the operation of particle accelerators by performing key functions including: Data acquisition, implementing control logic and safety interlocks, real-time processing of input/output signals and providing an interface for operator communications.

The intermediate level of the control system is programmed using IEC 61131-3 LADDER language (Mazur et al., 2016). Pre-processing of IO parameters is performed in this layer. The pre-processing stage involves scaling, calibration, and the soft start/stop of parameters, as well as the implementation of preventive interlocks for the gas injection subsystem.

The higher-level of the control system, which serves as the operator interface of the system, is developed in the graphical programming language "G" (Kodosky, 2020). This layer presents system parameters in a an intuitive manner, including vacuum levels, temperatures, beam energy and power, insulating gas pressure, input power, and the operational status of subsystems (see Fig. 12). The LabVIEW's programming capabilities, the development environment of the "G" language, facilitates the visualization, storage, and transmission of data across various protocols.

National Instruments OPC (OLE for Process Control) and Profinet protocols facilitates communication between the various layers of the control system. The design of the operator interface emphasizes the provision of real-time data on system status, performance parameters, and diagnostic information, organized into distinct sections. This layout allows operators to interact efficiently with each subsystem through specific sections of the graphical user interface (GUI).

5 Conclusions

The implemented control system has effectively integrated operational parameters of the accelerator into a cohesive interface, facilitating seamless monitoring and management. This system enables precise control over the electron beam irradiation process and allows for the dynamic adjustment of operational parameters. Currently, the control system is successfully operating under testing conditions of 500 kV and 10 mA. The architecture and design choices not only enhance user interaction but also ensure compliance with safety standards, thereby contributing to the overall efficiency and reliability of the accelerator's operation. Future developments will focus on further optimizing system performance and expanding its capabilities to accommodate a wider range of experimental applications.

Conflict of Interest

The authors declare no potential conflict of interest regarding the publication of this work.

References

Hasanpour, O., Abbasi Davani, F., Ghasemi, F., et al. (2022). Replacement of SF_2 with N_2/CO_2 in design of a parallel-fed voltage multiplier for electrostatic accelerator. *Radiation Physics and Engineering*, 3(2):17–25.

Kodosky, J. (2020). Labview. *Proceedings of the ACM on Programming Languages*, 4(HOPL):1–54.

Kuksanov, N. K., Salimov, R. A., Fadeev, S. N., et al. (2018). Current status of DC high power ELV electron accelerators. *Electrotechnica & Electronica (E+ E)*, 53.

Mazur, P., Chmiel, M., and Czerwinski, R. (2016). Central processing unit of IEC 61131-3-based PLC. *IFAC-PapersOnLine*, 49(25):454–459.

Nazari, M., Abbasi, F., Ghasemi, F., et al. (2016a). Design and simulation of a thermionic electron gun for a 1 MeV parallel feed Cockcroft-Walton industrial accelerator. In *7th Int. Particle Accelerator Conf.(IPAC'16), Busan, Korea, May 8-13, 2016*, pages 1976–1978. JACOW, Geneva, Switzerland.

Nazari, M., Abbasi, F., Ghasemi, F., et al. (2016b). Design, Simulation and Comparison of Electrostatic Accelerating Tubes for a 1 MeV Parallel Feed Cockcroft-Walton Industrial Accelerator. In *7th Int. Particle Accelerator Conf.(IPAC'16), Busan, Korea, May 8-13, 2016*, pages 1979–1981. JACOW, Geneva, Switzerland.

Nazari, M., Ghasemi, F., Abbasi, F., et al. (2020). Design and simulation of a 1 MeV, 100 mA parallel-fed capacitive coupled cascade industrial accelerator. *Journal of Instrumentation*, 15(01):T01001.

Sadeghche, Z., Ebrahimibasabi, E., Salehi, M., et al. (2023). Design and construction of voltage measurement instrument (GVM) for 1.5 MV dynamitron accelerator. *Iranian Journal of Physics Research*, 22(4):861–869.

Singh, S. et al. (2010). Particle accelerator control system. In *Proceedings of the DAE Symp. on Nucl. Phys*, volume 55, page I18.

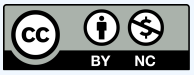

To cite this article:

Shirshekan, M., Hasanpour, O., Sadafi Biabli, M., Sanaye Hajari, S., Mohammadi, A., Nazari, M., Ghasemi, F. and Asl Beigi, M. (2025). Implementation of a control system for a laboratory-scale 1 MeV/25 kW electrostatic accelerator for irradiation experiments. Radiation Physics and Engineering, 6(2), 35-40. doi: 10.22034/rpe.2024.459998.1196

DOI: 10.22034/rpe.2024.459998.1196

To link to this article: https://doi.org/10.22034/rpe.2024.459998.1196